Channel Modeling of Wireless Networks in Tunnels

Zhi Sun and **Ian F. Akyildiz**

Broadband Wireless Networking Laboratory (BWN Lab)
School of Electrical & Computer Engineering, Georgia Institute of Technology, Atlanta, GA, 30332, USA
Email: {zsun; ian}@ece.gatech.edu

***Abstract*—The propagation characteristics of electromagnetic (EM) waves in tunnels are significantly different from those in terrestrial environment. However, the current tunnel channel models cannot provide an analytical solution for both near and far region of the sources. In this paper, the Multimode model is proposed to completely characterize the wireless channel of tunnels in roads/subways as well as underground mines. The new model provides an analytical expression for the path loss and delay spread at any position in a tunnel. This theoretical model is validated by comparing results with experiment measurements. Our channel model reveals that: the mode attenuation is mostly determined by the tunnel size and operating frequency, while the mode intensity is governed by the position of the transmission antenna. Physical factors, such as, humidity, pressure and temperature of the tunnel air, as well as the material of tunnel walls have little influence on the signal propagation in tunnels.**

I. Introduction

Reliable and efficient communication networks are urgently needed to improve the safety and productivity in underground mines, to realize convenient communication for drivers and passengers in road/subway tunnels, and to avoid terroristic attacks by surveilling those vulnerable areas. Compared with wire-based systems, wireless networking using natural wave propagation is a more flexible and efficient solution because it is low-cost, easy to implement and scalable [1], [2]. However, radio waves do not propagate well in tunnels [3]. Due to the bounding of tunnel walls, the propagation characteristics of electromagnetic (EM) signals are very different than in terrestrial wireless channels. To design an optimal wireless communication network in tunnels, an accurate channel model with realistic computational cost is needed to predict the path loss as well as the signal delay spread.

Currently there are mainly three techniques to model the channel characteristics of natural wave propagation in tunnels [4]: the Geometrical Optical model (GO model), the Waveguide model and the Full Wave model. In the GO model [5], [6], the EM field in the tunnel is obtained by summing the contributions of rays undergoing reflections on the tunnel walls and diffractions near tunnel wedges. It can numerically predict the path loss and signal delay at any position. However, the GO model requires a large amount of information to describe the environment [7]. Additionally, for long tunnel paths, the very large number of rays leads to numerical difficulties and the convergence may become very long. The waveguide model [8], [9], [10] considers a tunnel as an oversized waveguide with imperfectly lossy walls. Because the signal of higher order mode attenuates much faster than in the lower case, the waveguide model assumes there is only the lowest mode signal propagation in the tunnel. However, since the operating frequency (UHF) is much higher than the cut-off frequency in tunnels, the large number of modes will be exited near the transmitter antenna. Consequently, the waveguide model can not characterize the multi-mode operating channel in the near region. As a result, it can not be utilized in high density networks, e.g. wireless sensor networks. The full wave model, such as finite-difference time-domain (FDTD) techniques [11], completely models Maxwell's equations. This model provides very accurate results in arbitrary geometries. However, the model is limited to numerical result and also may create unrealistic computational burden even for a short tunnel path.

In this paper, we develop the Multimode model to analytically characterize the natural wave propagation in both near and far regions of the sources. In particular, we implement the GO model to analyze the field distribution of excitation plane, i.e. the tunnel cross-section that contains the transmitter antenna. This model does not have high computational cost because the analysis of the rays near the transmitter is limited to 2-dimensions. Then we use a mode-matching technique to match the modes' field derived by waveguide model to the field distribution derived by GO model. After that, we calculate the analytical results of each mode's intensity by numerical integration and non-linear regression. Finally, we predict the path loss and RMS delay spread at any position in a tunnel by utilizing the mode intensity and the waveguide model. We validate the proposed theoretical model by comparing results with experimental measurements. Based on the new channel model, we present an in-depth analysis on the tunnel wireless channel characteristics, which is influenced by multiple factors including operating frequency, tunnel size, antenna position and polarization for both transmitter and receiver, and dielectric properties of the tunnel walls and the tunnel air.

Our Multimode model is applicable to the tunnels in roads/subways as well as underground mines. It should be noted that this model is suitable for the mines using the longwall technique that is dominant in the USA and China. However, it is not accurate for most of the mines in Europe that use room and pillar mining method.

The remainder of this paper is organized as follows. In Section II, the Multimode model is developed in detail. Then,

† This work was supported by the US National Science Foundation (NSF) under Grant No. CCF-0728889.

978-1-4244-2324-8/08/$25.00 © 2008 IEEE.

This full text paper was peer reviewed at the direction of IEEE Communications Society subject matter experts for publication in the IEEE "GLOBECOM" 2008 proceedings.

in Section III, the characteristic of the tunnel wireless channel is analyzed by the new model. Finally, the paper is conclued in Section IV.

II. The Multimode Model

In this section, we introduce the Multimode model, which can be viewed as a multi-mode operating waveguide model. Because the modes worked out by the waveguide model are actually all possible solutions of the Maxwell's equations, only EM waves that have the same shapes as those modes are possible to exist in the tunnel. However, the intensity of each mode depends on the excitation, which can not be given by the waveguide model. Therefore, the GO model is involved to analyze the EM field distribution of the excitation plane. This field distribution can be considered as the weighted sum of the field of all modes. Hence, the intensity of each mode can be estimated by a mode-matching technique. Once the mode intensity is determined in the excitation plane, the propagation of each mode is mostly governed by the tunnel itself. Hence, the EM field of the rest of the tunnel can be accurately predicted by summing the EM field of each mode.

The remainder of this section is organized as follows. In Section II-A, the tunnel environment model is described. In Section II-B, the EM field distribution of the excitation plane is analyzed by the GO model. In Section II-C, a mode-matching technique is presented to match the EM fields of all possible modes in the excitation plane. In Section II-D, an analytical solution is provided to predict the path loss and delay spread. In Section II-E, the proposed channel model is validated by comparing our results with experiment measurements.

A. Tunnel Environment Model

Actual tunnel cross sections are generally in-between a rectangle and a circle. However, the EM field distribution and attenuation of the modes in rectangle waveguide are almost the same as the circular waveguide [2]. Hence, in our model, the tunnel cross section is treated as an equivalent rectangle with a width of $2a$ m and a height of $2b$ m. A Cartesian coordinate system is set with its origin located at the center of the rectangle tunnel. k_v, k_h and k_a are the complex electrical parameters of the tunnel vertical/horizontal walls and the air in the tunnel, respectively, which are defined as:

$$k_v = \varepsilon_0\varepsilon_v + \frac{\sigma_v}{j\omega}, \quad k_h = \varepsilon_0\varepsilon_h + \frac{\sigma_h}{j\omega}, \quad k_a = \varepsilon_0\varepsilon_a + \frac{\sigma_a}{j\omega} \quad (1)$$

where, ε_v, ε_h and ε_a are the relative permittivity for vertical/horizontal walls and the air in the tunnel; ε_0 is the permittivity in vacuum space; σ_v, σ_h and σ_a are their conductivity; ω is the angular frequency of the signal. The three areas are assumed to have the same permeability μ_0. The wave number in the tunnel space is given by:

$$k = \omega\sqrt{\mu_0\varepsilon_0\varepsilon_a} \quad (2)$$

We define the relative electrical parameter $\overline{k_v}$ and $\overline{k_h}$ for concise expression, which is:

$$\overline{k_v} = \frac{k_v}{k_a}, \qquad \overline{k_h} = \frac{k_h}{k_a} \quad (3)$$

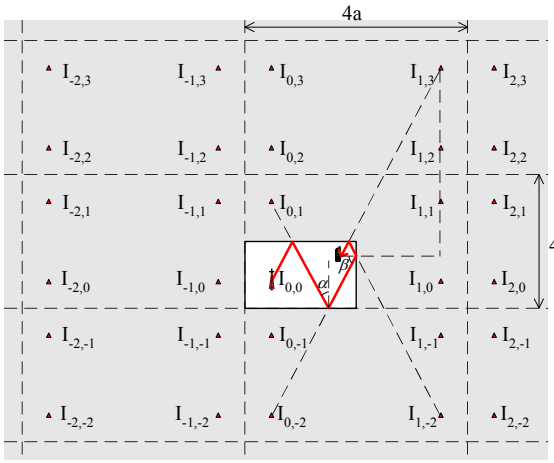

Fig. 1. The set of images in the excitation plane in a rectangular tunnel.

B. Field Analysis of Excitation Plane by GO Model

We assume that the transmitter antenna is a X-polarized electrical dipole. The results for Y-polarized antenna can be obtained simply by interchanging the x- and y-axes. The major polarized field plays a dominant role inside the tunnel and the coupling term can be omitted. Hence, in our Multimode model, we only need to match the major polarized fields of the GO model and the waveguide modes. The total field of a point in the excitation plane is equal to the sum of ray contributions from all reflection images added to that of the source. The reflection images are located as Fig 1 shows. Due to the geometry characteristic of rectangle cross section shape, the images and the reflection rays have the following properties:

- The ray coming from image $I_{p,q}$ experiences $|p|$ times reflection from the vertical wall and $|q|$ times reflection from the horizontal wall.
- Suppose that α is the incident angle on the horizontal wall, and β is the incident angle on the vertical wall. Then α and β are complementary. These angles remain the same for all reflections of a certain ray.

Consider that the transmitter antenna is located at the coordinate (x_0, y_0). The major polarized field, i.e. the X-polarized field, at the receiver is given by:

$$E_x^{Rx} = E_x^{Tx} \cdot \sum_{p,q} \left[\frac{\exp(-jkr_{p,q})}{r_{p,q}}\right] \cdot S(\overline{k_v})^{|p|} \cdot R(\overline{k_h})^{|q|} \quad (4)$$

where, E_x^{Tx} and E_x^{Rx} are the electric field at the transmitter and the receiver respectively; $r_{p,q}$ is the distance between image $I_{p,q}$ and the receiver; $R(\overline{k_h})$ and $S(\overline{k_v})$ are the reflection coefficients on the horizontal and vertical walls.

C. Mode-Matching in Excitation Plane

The major field eigenfunctions of X-polarized modes $E_{m,n}^x$ are given by [8]. It has been pointed out that the modes in a rectangle tunnel are approximately orthogonal [7], [12], i.e.

$$\int_{-a}^{a}\int_{-b}^{b} E_{m,n}^x \cdot E_{j,k}^{x^*}\, dxdy \simeq \begin{cases} \xi^2, & \text{if } m=j \text{ and } n=k \\ 0, & \text{otherwise} \end{cases} \quad (5)$$

This full text paper was peer reviewed at the direction of IEEE Communications Society subject matter experts for publication in the IEEE "GLOBECOM" 2008 proceedings.

where ξ is the norm of the modes.

The field of the modes can be viewed as a basis that spans the total field. Therefore, the mode intensity C_{mn} can be calculated by projecting the field of excitation plane obtained by the GO model $\left(E_x^{Rx}\text{ in (4)}\right)$ on the basis function $E_{m,n}^x$:

$$C_{mn} = \int_{-a}^{a}\int_{-b}^{b} E_x^{Rx} \cdot E_{m,n}^x \, dx\, dy \tag{6}$$

D. Analytical Solution for Multimode Model

Substitute (4) into (6) and change the sequence of summation and integration,

$$C_{mn} = \sum_{p,q}\left[\int_{-a}^{a}\int_{-b}^{b} E_x^{Rx}(p,q) \cdot E_{m,n}^x \, dx\, dy\right] \tag{7}$$

where, $E_x^{Rx}(p,q)$ is the field contributed by image $I_{p,q}$,

$$E_x^{Rx}(p,q) = E_x^{Tx} \cdot \frac{\exp(-jkr_{p,q})}{r_{p,q}} \cdot S(\overline{k_v})^{|p|} \cdot R(\overline{k_h})^{|q|} \tag{8}$$

Then the mode intensity C_{mn} can be viewed as the sum of all images' contributions: $C_{mn} = \sum_{p,q\in\mathbf{Z}} C_{mn}^{(p,q)}$, where,

$$C_{mn}^{(p,q)} = \int_{-a}^{a}\int_{-b}^{b}\Big\{E_x^{Tx} \cdot \frac{\exp(-jkr_{p,q})}{r_{p,q}} \cdot S(\overline{k_v})^{|p|} \cdot R(\overline{k_h})^{|q|} \cdot E_{m,n}^x\Big\} dx\, dy \tag{9}$$

Divide the absolute mode intensity by the norm of the basis ξ and the field of reference position $E_x(r_0)$ (r_0 apart from the antenna), then we can obtain the normalized mode intensity:

$$\begin{aligned}\overline{C_{mn}^{(p,q)}} &= \frac{C_{mn}^{(p,q)}}{\xi \cdot E_x(r_0)} = \frac{C_{mn}^{(p,q)}}{\xi \cdot E_x^{Tx} \cdot \frac{\exp(-jkr_0)}{r_0}} \\ &\simeq \frac{1}{\xi}\int_{-a}^{a}\int_{-b}^{b} \frac{r_0\exp(-jkr_{p,q})}{r_{p,q}+r_0} S(\overline{k_v})^{|p|} R(\overline{k_h})^{|q|} \cdot E_{m,n}^x \, dx\, dy\end{aligned} \tag{10}$$

The closed form solution of (10) is derived by composite numerical integration, which is given by:

$$\overline{C_{mn}^{(p,q)}} \simeq \frac{4}{3}\frac{\sqrt{ab}}{mn}\sum_{u=0}^{m-1}\sum_{v=0}^{n-1}\Big\{\frac{r_0\exp(-jkr_{p,q})}{r_{p,q}+r_0} S(\overline{k_v})^{|p|} R(\overline{k_h})^{|q|} \cdot(-1)^{\left\lfloor\frac{m+n}{2}\right\rfloor+1+u+v}\Big\} \tag{11}$$

The mode intensity is the summation of all images' contributions, however only the low-order images have significant effect. Specifically, for X-polarized field, only images $I_{p,q}$ with subscript p=$0,\pm1$ and q=$0,\pm1,\pm2$ are considered. In addition, to reduce the computation cost, the reflection coefficients R and S are simplified to their approximate expressions by non-linear regression. Therefore, the normalized intensity for mn-order mode is:

$$\overline{C_{mn}} \simeq \frac{4}{3}\frac{\sqrt{ab}}{mn}\sum_{\substack{p=0,\pm1\\q=0,\pm1,\pm2}}\Big\{\sum_{u=0}^{m-1}\sum_{v=0}^{n-1}\Big[\frac{r_0\exp(-jkr_{p,q})}{r_{p,q}+r_0} S^{|p|}R^{|q|} \cdot(-1)^{\left\lfloor\frac{m+n}{2}\right\rfloor+1+u+v}\Big]\Big\} \tag{12}$$

where,

$$R^{|q|} = (-1)^{|q|}\exp\big(-2|q|\cdot\frac{y_q}{r_{p,q}\sqrt{\overline{k_h}}}\big)$$

$$S^{|p|} = \begin{cases}1, & \text{if } p=0\\ 1-2\cdot\frac{1}{1+\frac{x_p}{r_{p,q}}\sqrt{\overline{k_v}}}, & \text{if } p=\pm1\end{cases}$$

$$x_p = \begin{cases}\left|2pa - x_0 + a - \frac{2a}{m}(u+\frac{1}{2})\right|, & \text{if } p \text{ is odd}\\ \left|2pa + x_0 + a - \frac{2a}{m}(u+\frac{1}{2})\right|, & \text{if } p \text{ is even}\end{cases}$$

$$y_q = \begin{cases}\left|2qb - y_0 + b - \frac{2b}{n}(v+\frac{1}{2})\right|, & \text{if } q \text{ is odd}\\ \left|2qb + y_0 + b - \frac{2b}{n}(v+\frac{1}{2})\right|, & \text{if } q \text{ is even}\end{cases}$$

$$r_{p,q} = \sqrt{x_p^2+y_q^2}$$

Then the predicted field at any position (x,y,z) inside the tunnel can be obtained by summing up the field of all significant modes at that position, which is given by:

$$E_x^{Rx}(x,y,z) = E_x(r_0)\sum_{m,n}\overline{C_{mn}}\cdot E_{m,n}^x(x,y)\cdot e^{-(\alpha_{mn}+j\beta_{mn})\cdot z} \tag{13}$$

where, α_{mn} is the attenuation coefficient and β_{mn} is the phase-shift coefficient [3], [9], [8]:

$$\begin{aligned}\alpha_{mn} &= \frac{1}{a}\left(\frac{m\pi}{2ak}\right)^2 Re\frac{\overline{k_v}}{\sqrt{\overline{k_v}-1}} + \frac{1}{b}\left(\frac{n\pi}{2bk}\right)^2 Re\frac{1}{\sqrt{\overline{k_h}-1}}\\ \beta_{mn} &= \sqrt{k^2-\left(\frac{m\pi}{2a}\right)^2-\left(\frac{n\pi}{2b}\right)^2}\end{aligned} \tag{14}$$

Similarly, the predicted received signal power at the coordinate (x,y,z) is given by:

$$P_r(x,y,z) = P_tG_tG_r \times\left(\frac{1}{2kr_0}\sum_{m,n}\overline{C_{mn}}\cdot E_{m,n}^x(x,y)\cdot e^{-(\alpha_{mn}+j\beta_{mn})\cdot z}\right)^2 \tag{15}$$

where, P_t is the transmitting power; G_t and G_r are the antenna gains of the transmitter and the receiver, respectively.

The propagation delay of EH_{mn} mode is $\tau_{(mn)}=z/v_{g(mn)}$, where $v_{g(mn)}$ is the group velocity that is given by $v_{g(mn)} = c^2\beta_{mn}/2\pi f$. The RMS delay spread τ_{rms} is the standard deviation of the delay of all the modes, weighted proportional to the mode power:

$$\tau_{rms}^2 = \frac{\sum_{m,n}(\tau_{(mn)}-\tau_m)^2\ P_{mn}(x,y,z)}{\sum_{m,n}P_{mn}(x,y,z)} \tag{16}$$

where, τ_m is the mean propagation delay at the position (x,y,z), and $P_{mn}(x,y,z)$ is the power coefficient of EH_{mn} mode at the position (x,y,z), given by:

$$P_{mn}(x,y,z) = \left|\overline{C_{mn}}\cdot E_{m,n}^x(x,y)\cdot e^{-\Gamma_{mn}^x\cdot z}\right|^2 \tag{17}$$

E. Comparison with Experimental Measurements

To validate the Multimode model, we compare our theoretical results with the experimental measurements provided in [1]. Using the same parameters, the received power at the frequency of $450\ MHz$, $900\ MHz$ and $2.1GHz$ is calculated by Multimode model, which is compared with the measurements

This full text paper was peer reviewed at the direction of IEEE Communications Society subject matter experts for publication in the IEEE "GLOBECOM" 2008 proceedings.

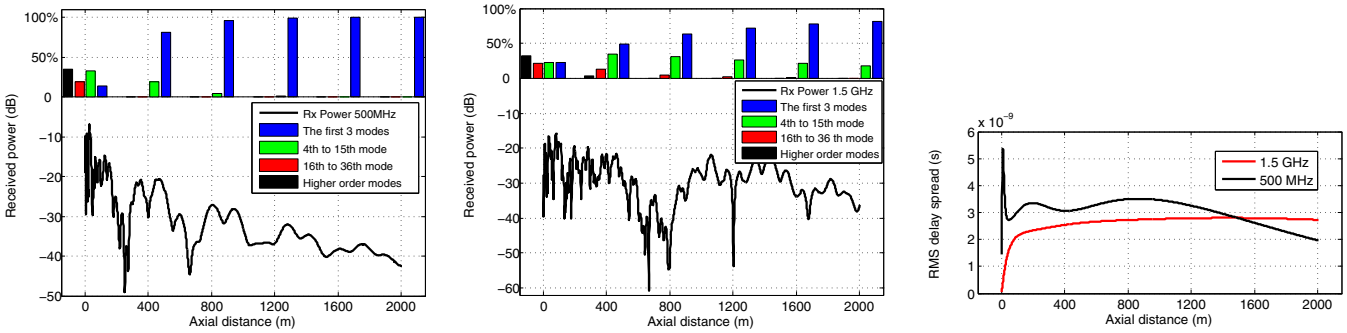

(a) Received signal power and the power distribution among modes at 500 MHz.

(b) Received signal power and the power distribution among modes at 1.5 GHz.

(c) RMS delay spread at 500 MHz and 1.5 GHz.

Fig. 2. Channel characteristics at different operating frequencies.

in [1, Fig 18], [1, Fig 19]. It is shown that the curves of the theoretical and experimental results are close to each other. Our Multimode model accurately predicts the attenuation velocity, the fast fading in the near region, the flat fading in the far region and the effects of different operating frequency.

III. Tunnel Wireless Channel Characteristics

In this section, the Multimode model is implemented to analyze the longitudinal attenuation and RMS delay spread under various tunnel conditions. Except studying the effect of certain parameters, default values are set as follows: The tunnel cross section shape is a rectangle with a height of 6 m and a width of 10 m; the tunnel wall, ceiling and floor are made of the same material with electrical parameter $\varepsilon = 5\varepsilon_0$, $\sigma = 0.01\ S/m$; the tunnel interior is filled with normal air ($\varepsilon = \varepsilon_0$, $\sigma = 0\ S/m$). The transmitting and receiving antennas are horizontal polarized dipoles at the same height (one-third of the tunnel height). Both antennas are placed at the same horizontal position of one-quarter of the tunnel width.

A. Operating Frequency

Fig 2 illustrates the effects of operating frequency on the channel characteristics. In the near region, the received power attenuates fast and fluctuates very rapidly. This is attributed to the combined effect of multiple modes. While in the far region, the fall in the received power is gradual. This is due to the fact that the higher order modes attenuate very fast as the distance increases. Hence, the field in the far region is governed by the few low-order modes left. The relationship between power distribution among modes and the received power is shown in Fig 2(a) and Fig 2(b). Although the operating frequency does not affect the power distribution of modes significantly, it has an obvious influence on the propagation constants. Signals with higher frequency attenuate slower. Hence, as frequency increases, the signal attenuation decreases and the fast fluctuating region is prolonged, as shown in Fig 2(b).

Fig 2(c) shows that the delay spread increases rapidly in the region very near the transmitter. There exists a turn point after which the rising speed of delay spread greatly drops down and negative growth may happen at long distance.It is because that RMS delay spread is caused by the different group velocity of different mode. In the very near region, multiple modes have comparable power; while in the far region, lower order modes become dominant. Because higher operating frequency has higher group velocity, the signal delay and delay spread are correspondingly smaller.

B. Tunnel Size

The tunnel size has similar effects on the channel characteristics as the operating frequency. In larger dimension tunnels, the attenuation constant α_{mn} is smaller and more mode remains significant in the far region. Therefore, the fast fluctuating region is prolonged in larger tunnels, and vice versa. For horizontal polarized antennas, the tunnel width plays a more important role because the reflection coefficients on the horizontal walls is larger than those on the vertical walls. Hence, the signal attenuates slower and fluctuates longer in larger and wider tunnels for horizontal polarized antenna. Similarly, in larger and higher tunnels, the power of all the modes drops down slower for vertical polarized antenna.

C. Antenna Position and Polarization

In Fig 3, we give the received power and power distribution among modes with different antenna position and polarization. In Fig 3(a), we show the case that the transmitter antenna is placed near the center of the tunnel cross section. The receiver antenna is placed either at the center or at the marginal position that is one-eighth of the tunnel height and one-eighth of the width. It is shown that the lowest modes are effectively excited (over 50% of the total power). If the receiver is also at the center, both the signal attenuation and the fluctuation are small. If the receiver is placed near the tunnel walls, the attenuation and fluctuation are much more significant. In Fig 3(b), we show the case that the transmitter antenna is placed near the tunnel wall ($1/8$ of the width and $1/8$ of the height). The receiver antenna is also placed either at the center or at the margin of the tunnel. Near the excitation plane, high order modes play the dominant role (over 80% of the total power). In this case, the position of receiver antenna does not affect the received signal as much as the former case. The attenuation

978-1-4244-2324-8/08/$25.00 © 2008 IEEE.

This full text paper was peer reviewed at the direction of IEEE Communications Society subject matter experts for publication in the IEEE "GLOBECOM" 2008 proceedings.

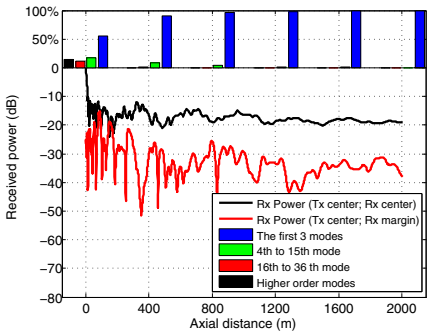

(a) Received signal power and the power distribution among modes when Tx antenna is placed near the tunnel center.

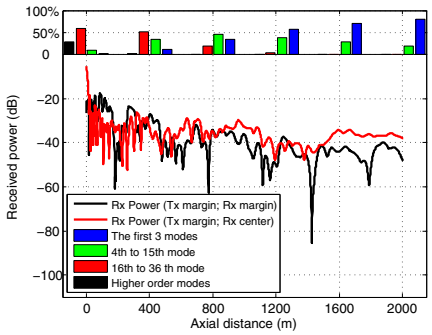

(b) Received signal power and the power distribution among modes when Tx antenna is placed near the tunnel wall.

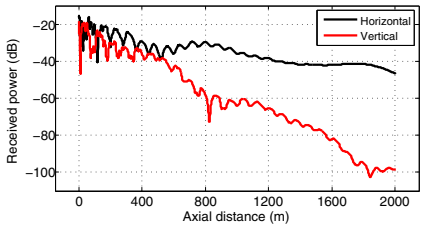

(c) Received signal power of different antenna polarization.

Fig. 3. Channel characteristics with different antenna position and polarization.

and fluctuation of received power is significant, no matter where the receiver is placed. In Fig 3(c), different antenna polarization is analyzed. To make the effect more obvious, we choose a wide but low tunnel ($10\times3\ m^2$) here. It is shown that the signal excited by horizontal polarized antenna attenuates much slower than that exited by vertical polarized antenna.

D. Electrical Parameters

The electrical parameters consist of permittivity ε and conductivity σ. The temperature, humidity and pressure have little influence on the air permittivity but may affect the conductivity more. However, the effect of different conductivity of tunnel air may be neglectable, because it is very small compared to the permittivity. Therefore, the electrical parameters of tunnel air can be considered the same as those of normal air. Tunnel walls' electrical parameters can be looked up in [3], where the permittivity of tunnel materials are in the range of $5\varepsilon_0 \sim 10\varepsilon_0$ and the conductivity is on the order of $10^{-2}\ S/m$ at the UHF frequency band. In this value range, the received power curves with different wall electrical parameters are very close to each other. Hence it can be concluded that the electrical parameters of either tunnel wall or tunnel air do not considerably influence the signal propagation inside the tunnel.

IV. Conclusion

Accurate channel model with realistic computational cost is needed to predict the wireless propagation characteristics in tunnels, which are greatly different from those in terrestrial wireless channels. Existing tunnel channel models do not provide an analytical solution for both near and far regions. In this paper, we develop the Multimode model to solve the problem. This model is applicable to the tunnels in roads/subways as well as underground mines. We first implement the GO model to analyze the field distribution of the excitation plane. This field is then projected to the orthogonal modes that is worked out by the waveguide model. The analytical expression of each mode's intensity is derived by mathematical approximation. The field at any position inside the tunnel can be predicted by the weighted sum of all significant modes where the weight is the mode's intensity. Based on the proposed channel model, our analysis shows that: on the one hand, the mode attenuation is mostly determined by the tunnel size and operating frequency, while the mode intensity is governed by the position of the transmission antenna. On the other hand, the humidity, pressure and temperature of the tunnel air, as well as the material of tunnel walls have little influence on the signal propagation in tunnels.

References

[1] D. G. Dudley, M. Lienard, S. F. Mahmoud and P. Degauque, "Wireless Propagation in Tunnels," *IEEE Antenna and Propagation Magazine*, vol. 49, no. 2, pp. 11-26, April 2007.

[2] M. Lienard and P. Degauque, "Natural Wave Propagation in Mine Environments," *IEEE Trans. on Antenna and Propagation*, vol. 48, no. 9, pp. 1326-1339, September 2000.

[3] P. Delogne, *Leaky Feeders and Subsurface Radio Communications*, Stevenage, Herts; New York: P. Peregrinus, August 1982

[4] C. Cerasoli, "RF Propagation in Tunnel Environments," In *Proceedings of IEEE Military Communications Conference, 2004 - MILCOM 2004*, vol. 1, pp. 363- 369, November 2004.

[5] S. F. Mahmoud and J. R. Wait, "Geometrical Optical approach for Electromagnetic Wave Propagation in Rectangular Mine Tunnels," *Radio Science*, vol. 9, no. 12, pp. 1147-1158, December 1974.

[6] Y. Hwang, Y. P. Zhang and R. G. Kouyoumjian, "Ray-Optical Prediction of Radio-Wave Propagation Characteristics in Tunnel Environments Part 1: Theory, Part 2: Analysis and Measurements" *IEEE Trans. on Antenna and Propagation*, vol. 46, no. 9, pp. 1328-1345, September 1998.

[7] D. Porrat, "Radio Propagation in Hallways and Streets for UHF Communications," *Ph.D Thesis*, Stanford University, 2002.

[8] K. D. Laakmann and W. H. Steier, "Waveguides: Characteristic Modes of Hollow Rectangular Dielectric Waveguides", *Applied Optics*, vol. 15, no. 5, pp. 1334-1340, May 1976.

[9] A. G. Emslie, R. L. Lagace and P. F. Strong, "Theory of the Propagation of UHF Radio Waves in Coal Mine Tunnels," *IEEE Trans. on Antenna and Propagation*, vol. AP-23, no. 2, pp. 192-205, March 1975.

[10] D. G. Dudley, "Wireless Propagation in Circular Tunnels," *IEEE Trans. on Antenna and Propagation*, vol. AP-53, no. 1, pp. 435-441, January 2005.

[11] A. Taflove and S. C. Hagness, *Computational Electrodynamics: The Finite-Difference Time-Domain Method*, 3rd ed. Norwood, MA: Artech House, 2005.

[12] J. M. Molina-Garcia-Pardo, M. Lienard, P. Degauque, D. G. Dudley and L. Juan-Llacer, "Interpretation of MIMO Channel Characteristics in Rectangular Tunnels from Modal Theory," *IEEE Trans. on Vehicular Technology*, to appear.